Elucidating Quantum Number-Dependent Coupling Matrix Elements Using Picosecond Time-Resolved Photoelectron Spectroscopy

Julia A. Davies* and Katharine L. Reid

School of Chemistry, University of Nottingham, Nottingham NG7 2RD, United Kingdom

(Received 21 May 2012; published 9 November 2012)

We measure quantum beating patterns of photoelectron intensity caused by intramolecular vibrational energy redistribution following the excitation of a low-lying ring breathing state in S_1 parafluorotoluene. Analysis of the beating patterns reveals an exceptional sensitivity to details of the evolving wave packet which is found to contain two incoherent components, one of which rapidly dephases. This analysis enables the determination of coupling matrix elements, which are shown to depend strongly on torsional and rotational quantum numbers.

DOI: 10.1103/PhysRevLett.109.193004 PACS numbers: 33.60.+q, 33.15.Mt, 33.20.Vq, 33.80.−b

Time-resolved photoelectron spectroscopy, in which a nonstationary state is prepared with a pump pulse and probed through ionization, has emerged as a powerful probe of intramolecular dynamics [1–5]. The time dependence of peaks in the photoelectron spectra has enabled signatures of nonadiabatic processes to be observed and excited state lifetimes to be determined. The vast majority of time-resolved photoelectron spectroscopy experiments are performed with femtosecond laser pulses, and as a consequence the resolution of the photoelectron spectra is limited by the laser bandwidth, which is typically >100 cm^{-1}. Although this presents no disadvantage for dynamical processes that are over in a few picoseconds, significantly more information can be obtained for longer time scale processes if photoelectron spectra are obtained at higher energy resolution using picosecond laser pulses. In earlier work on toluene and parafluorotoluene (*p*-fluorotoluene), we have observed sustained quantum beating patterns of energy-resolved photoelectron intensity over tens or hundreds of picoseconds [6,7]. This has been achieved through the use of laser pulses of 1 ps in duration with a bandwidth of $\sim$13 cm^{-1}, together with selective monitoring of relatively slow photoelectrons, thus allowing individual vibrational states to be resolved. This technique has enabled the identification of dark states that promote the redistribution of vibrational energy and the quantitative determination of coupling coefficients connecting zero-order vibrational states.

The *p*-fluorotoluene molecule (see inset of Fig. 1) has been used by several research groups as a prototype for studies aimed at investigating the role of attached internal rotors, in this case a methyl group, on intramolecular vibrational energy redistribution [7–10]. It has been observed that the presence of the rotor increases redistribution rates, and in some cases a specific role for torsion-vibration coupling has been established. At the typical temperature of a jet-cooled pulsed molecular beam ($\sim$ 10 K), approximately equal populations are prepared in internal rotor states with $|m| = 0$ and $|m| = 1$, where m is the internal rotational (or torsional) quantum number and $|m| = 1$ contains the degenerate pair $m = \pm 1$. This allows the vibrational dynamics in two incoherently prepared torsional states to be studied simultaneously. In this Letter we present results on the 1^1 vibrational state in S_1 *p*-fluorotoluene. The results indicate a significant interdependence of rotational, torsional, and vibrational degrees of freedom, which in turn is expected to provide a key mechanism for energy redistribution. To the best of our knowledge, this is the first observation of the influence of rotationally dependent Hamiltonian coupling matrix elements in time-resolved work.

A laser pulse of 1 ps in duration and 13 cm^{-1} bandwidth at a wavelength of 265.55 nm is used to prepare *p*-fluorotoluene in the 1^1 zero-order vibrational level of its S_1 electronic state, where the 1^1 level lies $\sim$798 cm^{-1} above the S_1 origin and mode 1 is a ring breathing motion. A second laser pulse, with the same duration, polarization and bandwidth, but tunable wavelength, is then used to ionize the evolving wave packet after a known time defined by a delay stage, and photoelectrons are detected in a velocity-map imaging spectrometer. Our experimental apparatus has been described in earlier work [6].

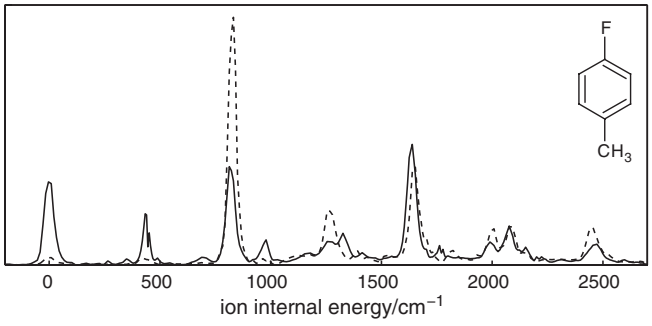

FIG. 1. Slow-electron velocity-map imaging spectrum obtained following excitation of the 1^1 bright state in S_1 *p*-fluorotoluene and measured at pump-probe time delays of 0 ps (solid line) and 2.5 ps (dashed line). The abscissa is positioned at zero intensity.

In Fig. 1 we show composite photoelectron spectra measured at time delays of 0 and 2.5 ps. Each spectrum, known as a "SEVI" (slow-electron velocity-map imaging) spectrum [11], has been generated by combining the photoelectron spectra taken at five different ionizing wavelengths to enable each peak in the spectrum to be optimally resolved; our photoelectron kinetic energy is typically less than 500 cm^{-1} and our resolution is ~40 cm^{-1}. Each spectrum provides a signature for the S_1 vibrational state from which ionization has occurred. The 0 ps spectrum originates from ionization of the S_1 1^1 "bright" zero-order state and the 2.5 ps spectrum is attributed to ionization of the S_1 $9b^2$ "dark" zero-order state [12], where $9b$ represents a CF rocking vibrational mode. The intensity of the $v = 0$ ion state at 0 cm^{-1} in Fig. 1 is reduced to almost zero at 2.5 ps indicating that this photoelectron peak can be used to map the evolution of the S_1 1^1 bright state. The dark state assignment to S_1 $9b^2$ has been assisted by quantum chemistry calculations reported in our previous work [7]. Both vibrational states are totally symmetric, suggesting that they are coupled through anharmonicity and therefore are in Fermi resonance.

In Fig. 2 we show the photoelectron intensity corresponding to the $v = 0$ ion state as the delay stage is scanned in steps of 0.5 ps; a probe wavelength of 298.8 nm is used to ensure that vibrationally excited states of the ion are not populated. The time-resolved beating pattern shows an oscillation with a period of ~5 ps that persists for at least 500 ps. A "fast decay" in the oscillation amplitude is observed between 0 to 30 ps and, in addition, the beating pattern reveals local minima in amplitude at ~37 and ~107 ps and a local maximum at ~73 ps. The Fourier transform of the data is shown in the inset to Fig. 2 and reveals two frequency components: an intense sharp feature centered at 6.69 cm^{-1} and a low intensity broad feature peaked at 6.22 cm^{-1}. By analogy with our earlier work [6], and following the rules required to analyze quantum beating patterns [13], we attribute these two frequencies to the energy separations, ΔE_{12} and $\Delta E'_{12}$, between two S_1 vibrational eigenstates ($|1\rangle$ and $|2\rangle$) in each of the two torsional channels (unprimed and primed) that are populated at a molecular beam temperature of 10 K. In each torsional channel the two eigenstates result from the coupling between the 1^1 and $9b^2$ zero-order vibrational states, according to $|1\rangle = \alpha_{1a}|a\rangle + \alpha_{1b}|b\rangle$ and $|2\rangle = \alpha_{2a}|a\rangle + \alpha_{2b}|b\rangle$, where $|a\rangle$ denotes the bright state (1^1), $|b\rangle$ denotes the dark state ($9b^2$), and the α's are m-dependent coupling coefficients that express the contribution of $|a\rangle$ and $|b\rangle$ to each eigenstate ($|1\rangle$ and $|2\rangle$). Although it is surprising that so few coupled vibrational states lie within the laser bandwidth at this excitation energy, this is the clear interpretation of the Fourier transform. The broad feature in the Fourier transform spectrum suggests that a spread of frequencies close to 6.22 cm^{-1} are present, which is a preliminary indication of substantial rotational dephasing for one torsional component of the prepared vibrational wave packet and is consistent with the "fast decay" in oscillation amplitude observed during the first 30 ps. In previous work, dephasing has been attributed to mismatches in the rotational constants associated with different zero-order vibrational states; however, this process would typically be expected to take

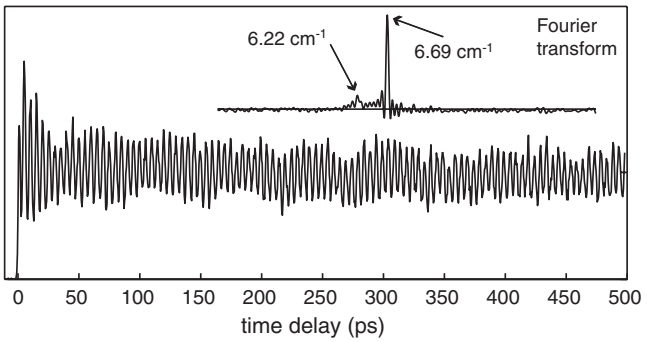

FIG. 2. Time-resolved photoelectron intensity corresponding to the $v = 0$ state in the ion measured as the delay stage is scanned from −20 to +500 ps (see text). The inset shows the Fourier transform of this data with a horizontal line indicating zero amplitude.

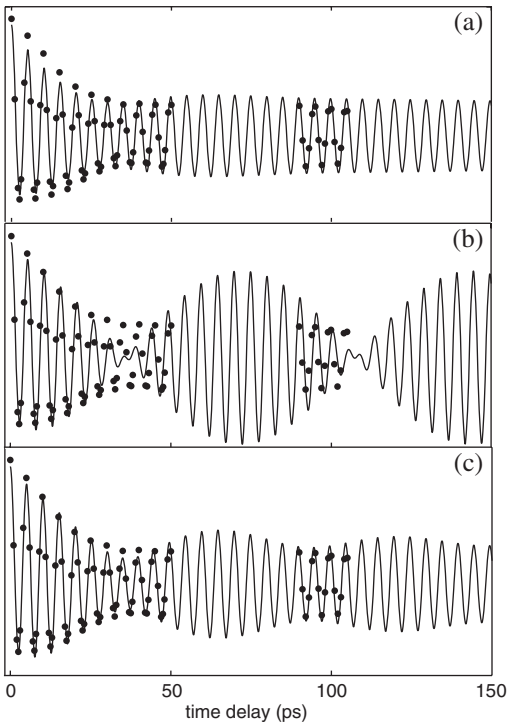

FIG. 3. In each panel the data points (solid circles) represent time-resolved photoelectron intensity corresponding to the $v = 0$ state in the ion obtained from analysis of the measured time-resolved photoelectron spectra. The solid line represents (a) an empirical fit of the data to Eq. (4), (b) a simulation based on Eq. (1) using the parameters given in Table I with no rotational dephasing of the vibrational wave packet, and (c) a simulation based on Eqs. (1) and (6). In both (b) and (c) an additional empirical correction term has been included (see text and Table I).

place over nanoseconds or hundreds of picoseconds for a molecular beam temperature of ~10 K [14,15] rather than the time scale of ~30 ps observed here.

In order to further investigate the "fast decay" in oscillation amplitude, it is necessary to obtain more accurate data at short time delays. For this purpose, we have measured photoelectron images at a series of time delays from 0 to 50 ps in 1 ps steps, plus additional data at selected time delays up to 500 ps, using data collection times that are 50 times longer than for the data shown in Fig. 2. For this experiment an ionizing wavelength of 284.3 nm was chosen, allowing the time profiles for vibrationally excited states to be measured in addition to the $v = 0$ state. Because no additional frequency components were observed in these additional time profiles we present data (solid circles) for the $v = 0$ peak only in Fig. 3. The time profile data reveal a smoothly varying oscillation amplitude that we will compare with simulated time profiles obtained using various models for the rotational dephasing process.

The $v = 0$ state of the ion has nonzero Franck-Condon overlap only with the bright state component of each eigenstate in the superposition prepared in S_1. Adapting the formalism of Felker and Zewail [13] we can express the time-dependent photoelectron intensity, $S(t)$, corresponding to such an ion state as follows:

$$\begin{aligned} S(t) \propto & \sum_{JK} P(J,K)\{{\alpha_{1a}}^4 + {\alpha_{2a}}^4 + 2{\alpha_{1a}}^2{\alpha_{2a}}^2\cos[\omega_{12}(J,K)t]\} \\ & + \sum_{JK} P'(J,K)\{{\alpha'_{1a}}^4 + {\alpha'_{2a}}^4 \\ & + 2{\alpha'_{1a}}^2{\alpha'_{2a}}^2\cos[\omega'_{12}(J,K)t]\} \\ = & \sum_{JK} P(J,K)\{C + D\cos[\omega_{12}(J,K)t]\} \\ & + \sum_{JK} P'(J,K)\{C' + D'\cos[\omega'_{12}(J,K)t]\}, \end{aligned} \tag{1}$$

where the primed and unprimed quantities refer to the two torsional components; all equations that are written in terms of the unprimed variables will also apply to the equivalent primed variables. In Eq. (1) the coefficient $P(J, K, m)$ gives the Boltzmann population of the (J, K) rotational level and the m internal rotation level.

From first order perturbation theory the eigenstate energy separations are given by

$$\Delta E_{12}(J,K) = \hbar\omega_{12}(J,K) = 2|V_{ab}(J,K)|(R_{JK}^2 + 1)^{1/2}, \tag{2a}$$

where

$$R_{JK} = \left| \frac{\Delta E_{ab}(J,K)}{2V_{ab}(J,K)} \right|. \tag{2b}$$

Here, ΔE_{ab} is the zero-order energy separation and V_{ab} is the Hamiltonian coupling matrix element that connects the bright state $|a\rangle$ (1^1) to the dark state $|b\rangle$ $(9b^2)$. In principle, from this equation, rotational dephasing can occur through either (i) a rotational dependence for ΔE_{ab} caused by differences in the rotational constants for the zero-order states $|a\rangle$ and $|b\rangle$, or (ii) a rotational dependence of the Hamiltonian coupling matrix element V_{ab}. However, if the zero-order states are coupled through anharmonicity, as they would be for a classic Fermi resonance, then the Hamiltonian coupling matrix will be independent of J, K and so any dephasing is expected to be caused by the former mechanism.

To proceed any further we need to deduce the rotationally averaged values of ΔE_{ab} and V_{ab} from our data. To achieve this we assume, for the time being, that the dephasing effect can be approximated by an exponential decay [14], and that the $m = 0$ and $|m| = 1$ torsional levels are equally populated [7]. In this case Eq. (1) becomes

$$\begin{aligned} S(t) \propto & C + C' + D\cos(\bar{\omega}_{12}t)\exp(-kt) \\ & + D'\cos(\bar{\omega}'t)\exp(-k't), \end{aligned} \tag{3}$$

where $\hbar\bar{\omega}_{12}$ and $\hbar\bar{\omega}'_{12}$ are the rotationally averaged eigenstate energy separations, $\Delta\bar{E}_{12} = \hbar\bar{\omega}_{12} = \sum_{JK} P(J,K)\Delta E_{12}(J,K)/\sum_{JK} P(J,K)$. According to Felker and Zewail [13], Eq. (3) can be used to yield quantitative dynamical information through the modulation depth of the beats, $M_a = 2\alpha_{1a}^2\alpha_{2a}^2/(\alpha_{1a}^4 + \alpha_{2a}^4) = D/C$, which is related to the rotationally averaged values of ΔE_{ab} and V_{ab} through the relationship $M_a = \frac{1}{(2\bar{R}^2+1)}$, where $\bar{R} = \sum_{JK} P(J,K)R_{JK}/\sum_{JK} P(J,K)$ and R_{JK} is given by Eq. (2b).

However, the representation of the data in the first 10 ps requires an additional exponential decay term to be added to Eq. (3) with a time constant of 7 ps; the need for this term suggests that an additional minor redistribution channel is contributing to the observed dynamics. The empirically corrected equation is therefore given by

$$\begin{aligned} S(t) \propto & C + C' + D\cos(\bar{\omega}_{12}t)\exp(-kt) \\ & + D'\cos(\bar{\omega}'_{12}t)\exp(-k't) + F\exp(-k_F t). \end{aligned} \tag{4}$$

With the inclusion of this final term we obtain an empirical fit to the data which is shown in Fig. 3(a). From the fit we determine that the modulation depths $M_a = D/C$ and $M'_a = D'/C'$ are comparable for the two torsional components, giving a torsionally averaged value of $\bar{M}_a = 0.97$. Using this value, along with the relationship given in Eq. (2), we are able to deduce rotationally averaged values for (i) coupling coefficients α, (ii) Hamiltonian coupling matrix elements V_{ab}, and (iii) zero-order energy separations ΔE_{ab}. These are listed in Table I.

We now consider the effect that an explicit rotational dependence of ΔE_{ab} would have on our observations by performing simulations at 10 K, using the rotationally averaged values as a starting point. For reference purposes, we first show the results of a simulation with no dephasing in Fig. 3(b); clearly this does not provide even a qualitative description of our observations. Next we consider the

TABLE I. Parameters deduced from the Fourier transform (Fig. 2) and the fit of the data shown in Fig. 3 to Eq. (4). The values of δ are those used in Eq. (6) to best model the data.

	Unprimed channel	Primed channel
$\Delta\bar{E}_{12}(\mathrm{cm}^{-1})$[a]	6.69	6.22
$\Delta\bar{E}_{ab}(\ \mathrm{cm}^{-1})$[a]	0.83	0.77
$\bar{V}_{ab}(\mathrm{cm}^{-1})$[a]	3.32	3.09
$\alpha_{1a} = \alpha_{2b}$	0.75	0.75
$\alpha_{2a} = -\alpha_{1b}$	−0.66	−0.66
δ	1×10^{-5}	3×10^{-4}
$F/S(0)$[b]	0.14	
$k_F\ (\mathrm{ps}^{-1})$[b]	0.143	

[a]Rotationally averaged values.
[b]Parameters associated with a minor incoherent channel, see Eq. (4).

effects caused by different values for the rotational constants in the coupled vibrational states. Because *p*-fluorotoluene has two similar moments of inertia we assume that it can be treated as a symmetric top rotor with rotational constants A and B, where B is given by the average of the B and C asymmetric rotor rotational constants. The starting values for these rotational constants were taken from the values determined by Cvitas and Hollas for the S_1 origin [16]. We use the subscript a or b to denote the dependence on the 1^1 or $9b^2$ zero-order vibrational state. Thus

$$\Delta E_{ab}(J,K) = \Delta E_{ab}(0,0) + \Delta B J(J+1) + (\Delta A - \Delta B)K^2, \tag{5}$$

where $\Delta B = B_b - B_a$ and $\Delta A = A_b - A_a$.

Using Eq. (5) we varied the rotational constants for $|a\rangle$ and $|b\rangle$ in each torsional channel in order to best represent the data by simulating the quantum beating patterns using Eq. (1) together with the empirical "F term" given in Eq. (4). Although it is possible to achieve a good match to the data using this approach, very large changes in rotational constant (or moment of inertia) are required, with the best simulation yielding a $\Delta B/B_a$ value of 1.5% for the "unprimed" torsional channel, and 53% for the "primed" channel. These values are much larger than those typically expected for aromatic molecules, in which rotational constants are estimated to vary by significantly less than 1% between zero-order vibrational states [14]. Furthermore, a 53% change in B would require a change in molecular geometry that is physically unrealistic. This provides clear evidence that the observed fast decay cannot be attributed to a vibrational level dependence of the rotational constants.

In order to investigate this further we leave ΔE_{ab} independent of (J, K) and instead model the rotational dependence by assuming that V_{ab} can be expressed by

$$V_{ab}(J,K) = V_{ab}(0,0) + \delta J(J+1)V_{ab}(0,0). \tag{6}$$

Using Eq. (6) we varied the value of δ for each torsional channel and substituted the resulting $V_{ab}(J, K)$ into Eq. (1) with the additional "F term" from Eq. (4). The best match to the experimental data is shown in Fig. 3(c), and uses the δ values given in Table I. This simulation clearly represents the data far better than the empirical fit [Fig. 3(a)] given by Eq. (4), not only in terms of quantitative agreement with the data in Fig. 3 for the initial "fast decay," but also in terms of qualitative agreement with the data in Fig. 2 because it faithfully reproduces the relative amplitudes of the minimum at ~37 ps and the maximum at ~73 ps. We note that no offsets have been applied in order to match the simulation to the data. The value of δ deduced for the primed channel gives a significant rotational dependence to $\Delta E'_{12}$, which suggests that the coupling is more complicated than originally anticipated; see below. The deduced value of δ for the unprimed torsional channel enables the observed photoelectron intensity near 500 ps (not shown in Fig. 3) to be correctly represented.

From our time-resolved data (Figs. 2 and 3), and the Fourier transform shown in the inset to Fig. 2, it is clear that the observations are dominated by the presence of two pairs of coupled zero-order states, apparently in Fermi resonance. However, the rotational dependence of V_{ab}, which is necessary to account fully for the observations, is inconsistent with a classic Fermi resonance. A possible explanation for this is that the 1^1 and $9b^2$ zero-order states are weakly coupled to additional dark states that either (i) lie outside the laser bandwidth or (ii) give rise to eigenstates with negligible oscillator strength. Application of the coupling selection rules for the two torsional channels [7] results in two distinct sets of candidate states that can couple to the primed and unprimed bright state, thus accounting for the different dynamics observed for the two torsional channels. Our results therefore suggest that additional states provide the means of adding an m-specific rotational dependence to a coupling element that is predominantly anharmonic; an observation analogous to this has been made in frequency-resolved work by Lehmann, Scoles, and coworkers [17]. Evidence of the involvement of additional states is also provided by the necessity of including the "F term," attributed to an additional redistribution channel, in both the simulation and fit.

We conclude that quantum beating patterns of energy-resolved photoelectron intensity in picosecond time-resolved experiments are highly sensitive both to coupling between zero-order vibrational states and to any rotational and torsional dependence of that coupling.

We are grateful to Colin Western and Warren Lawrance for helpful discussions. This work was supported by EPSRC Grant No. EP/E046150.

*Present address: Department of Chemistry, Imperial College London, Exhibition Road, London SW7 2AZ, U.K.

[1] T. Suzuki, Annu. Rev. Phys. Chem. **57**, 555 (2006).

[2] A. Stolow and J. G. Underwood, in *Advances in Chemical Physics*, edited by S. A. Rice (John Wiley & Sons. Inc., New York, 2008), Vol. 139, p. 497.
[3] C. Z. Bisgaard, O. J. Clarkin, G. Wu, A. M. D. Lee, O. Geßner, C. C. Hayden, and A. Stolow, Science **323**, 1464 (2009).
[4] O. Schalk, A. E. Boguslavskiy, A. Stolow, and M. S. Schuurman, J. Am. Chem. Soc. **133**, 16 451 (2011).
[5] Y.-I. Suzuki, T. Horio, T. Fuji, and T. Suzuki, J. Chem. Phys. **134**, 184313 (2011).
[6] J. A. Davies, A. M. Green, and K. L. Reid, Phys. Chem. Chem. Phys. **12**, 9872 (2010).
[7] J. A. Davies and K. L. Reid, J. Chem. Phys. **135**, 124305 (2011).
[8] C. S. Parmenter and B. M. Stone, J. Chem. Phys. **84**, 4710 (1986).
[9] D. B. Moss, C. S. Parmenter, and G. E. Ewing, J. Chem. Phys. **86**, 51 (1987).
[10] A. K. King, S. M. Bellm, C. J. Hammond, K. L. Reid, M. Towrie, and P. Matousek, Mol. Phys. **103**, 1821 (2005).
[11] A. Osterwalder, M. J. Nee, J. Zhou, and D. M. Neumark, J. Chem. Phys. **121**, 6317 (2004).
[12] J. A. Davies and K. L. Reid (unpublished).
[13] P. M. Felker and A. H. Zewail, J. Chem. Phys. **82**, 2961 (1985).
[14] P. M. Felker and A. H. Zewail, J. Chem. Phys. **82**, 2994 (1985).
[15] P. G. Smith and J. D. McDonald, J. Chem. Phys. **96**, 7344 (1992).
[16] T. Cvitas and J. M. Hollas, Mol. Phys. **20**, 645 (1971).
[17] J. E. Gambogi, E. R. Th. Kerstel, K. K. Lehmann, and G. Scoles, J. Chem. Phys. **100**, 2612 (1994).